SUPPORTING INFORMATION

Synthesis and biological evaluation of pyrazole-pyrimidones as a new class of correctors of the Cystic Fibrosis Transmembrane Conductance Regulator (CFTR)

Christian Vaccarin[1,2], Guido Veit[3], Tamas Hegedus[4,5], Odalys Torres[4], Adriana Chilin[1], Gergely L Lukacs[3]* and Giovanni Marzaro[1]*

[1]Department of Pharmaceutical and Pharmacological Sciences, University of Padova, 35131 Padova, Italy.
[2]Center for Radiopharmaceutical Sciences, ETH-PSI-USZ, Paul Scherrer Institute, 5232 Villigen, Switzerland.
[3]Department of Physiology and Biochemistry, McGill University, Montréal, QC, H3G 1Y6, Canada.
[4]Institute of Biophysics and Radiation Biology, Semmelweis University, 1085 Budapest, Hungary.
[5]HUN-REN Biophysical Virology Research Group, Hungarian Research Network, Budapest, 1052, Hungary.

***Corresponding Authors**: Giovanni Marzaro (giovanni.marzaro@unipd.it) and Gergely L. Lukacs (gergely.lukacs@mcgill.ca)

Table of Contents

Wt-CFTR conformation	Score of 4172 best pose (Kcal/mol)	Binding site of 4172 best pose	Score of 1 best pose (Kcal/mol)	Binding site of 1 best pose	Score of 10 best pose (Kcal/mol)	Binding site of 10 best pose
1	-9.8 (3)[a]	b	-9.7 (2)	a	-10.5 (7)	a
2	-9.1 (10)	a	-9.2 (6)	a	-9.9 (9)	a
3	-9.4 (7)	a	-9.0 (8)	a	-8.6 (10)	c
4	-9.8 (4)	c	-9.4 (4)	b	-11.9 (3)	b
5	-9.6 (6)	a	-9.5 (3)	b	-12.0 (2)	a
6	-10.0 (2)	b	-9.3 (5)	c	-11.8 (4)	b
7	**-10.7 (1)**	**b**	**-10.5 (1)**	**b**	**-12.1 (1)**	**b**
8	-9.3 (9)	b	-8.9 (9)	b	-10.9 (5)	a
9	-9.7 (5)	a	-9.2 (6)	a	-10.5 (7)	b
10	-9.4 (7)	c	-8.6 (10)	c	-10.7 (6)	b

Table S1. Lowest energy pose scores for compounds **4172**, **1** and **10** against each wt-CFTR. Protein conformations were derived from clusterization of all-atoms molecular dynamics. [a]The numbers between brackets indicate the overall rank of the score against the 10 conformations.

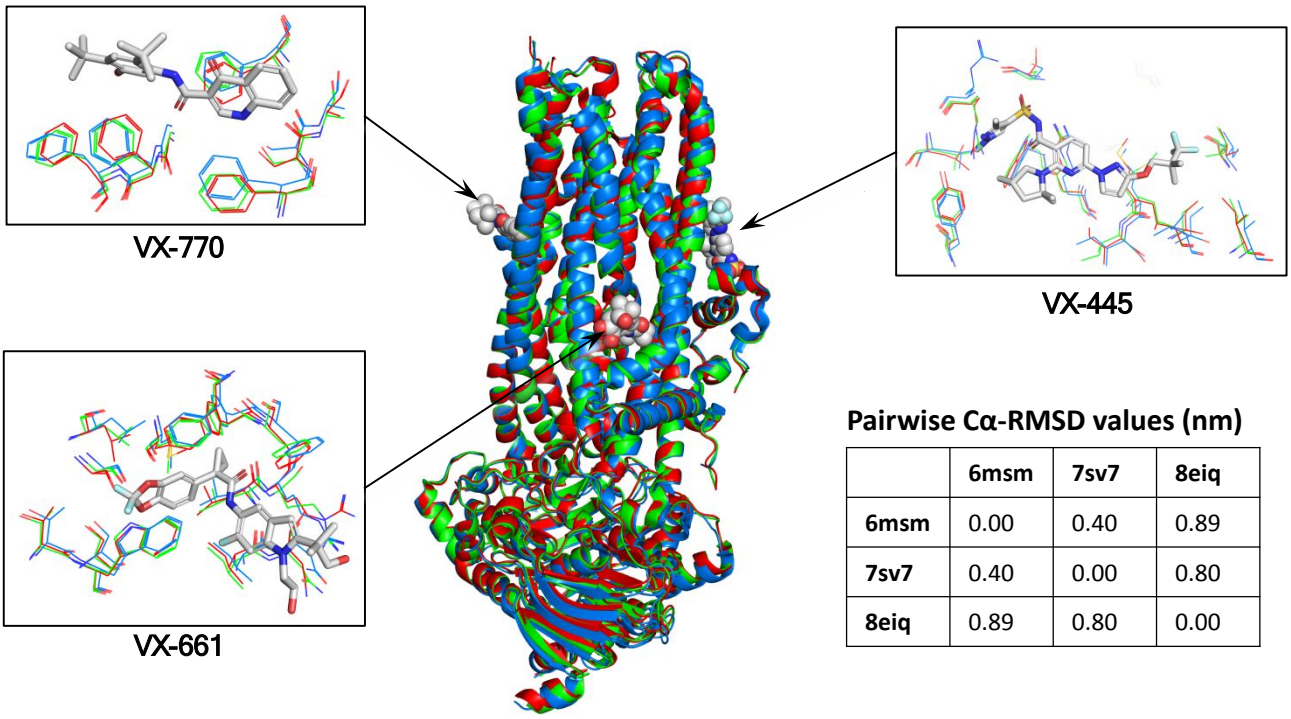

Pairwise Cα-RMSD values (nm)

	6msm	7sv7	8eiq
6msm	0.00	0.40	0.89
7sv7	0.40	0.00	0.80
8eiq	0.89	0.80	0.00

Figure S1. Superimposition of cryo-EM CFTR structures. PDB IDs: 6msm (red), 7sv7 (green), 8eiq (blue). Bound correctors (extracted from 8eiq) are highlighted as spheres. Later panels show the details of residues (showed as lines) surrounding VX-770, VX-445 and VX-661 (showed as sticks). Pairwise Cα-RMSD values calculated after superimposition of the three CFTR structures are also reported.

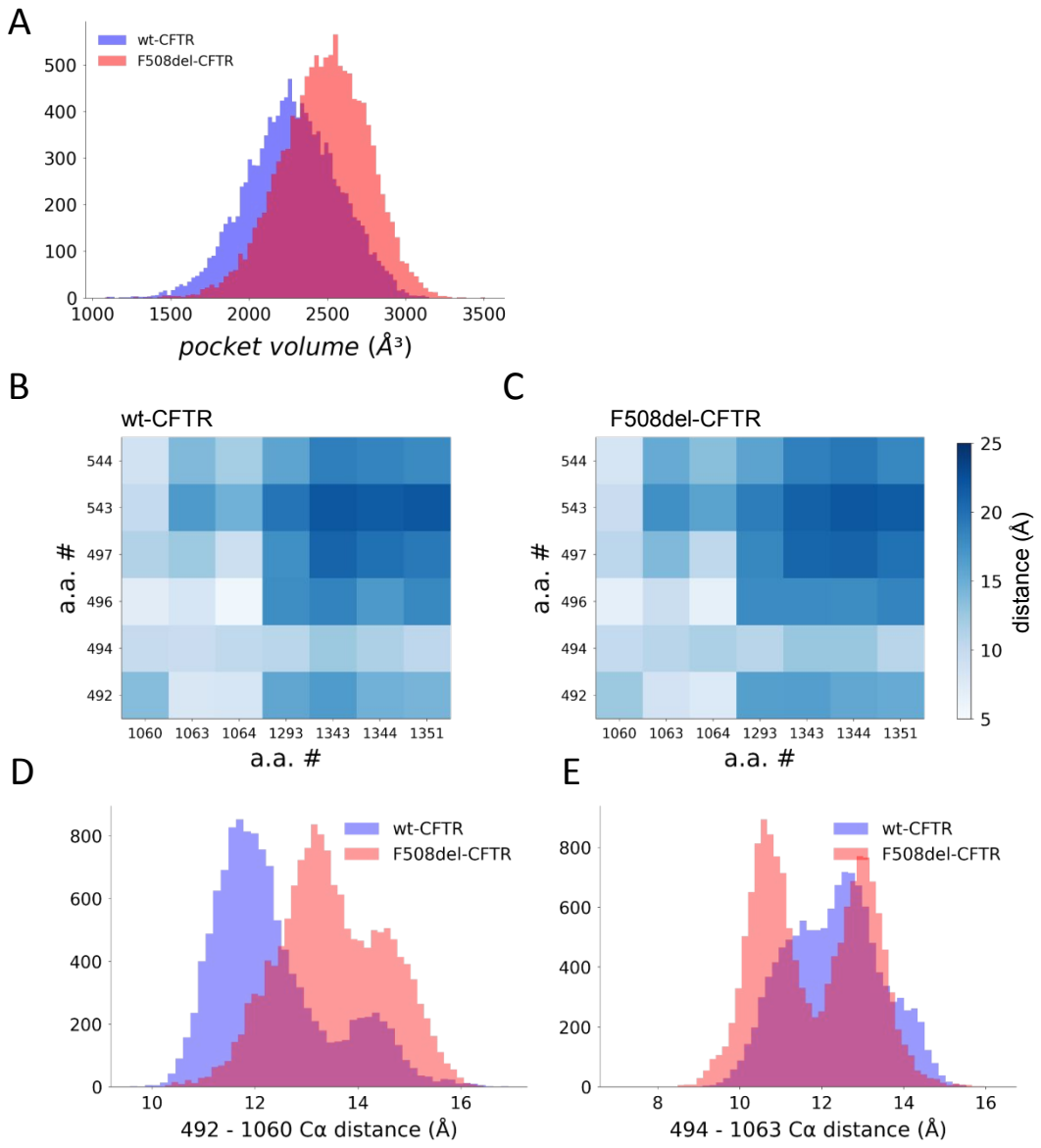

Figure S2. Results from molecular dynamics simulations. (A) The volume of the identified pocket "b" was increased in F508del compared to wild type. The pocket volume in the conformations merged from six trajectories (300-500 ns) was calculated using the MDpocket software. (B, C) The distance of NBD1 from NBD2 and CL4 is slightly increased upon F508del. The distance between the center of geometry of residues forming the pocket were calculated in frames from the sub-trajectories. The mean of the distance values were plotted. Residues within 4.5 Å from the docked molecule in the centroid structure were defined as pocket-forming residues (NBD1: 492, 494, 496, 497, 543, and 544; CL4: 1060, 1063, 1064, NBD2: 1293, 1343, 1344, 1351). (D, E) The increasing distance and pocket volume provides also space for amino acid side chains to flip into the pocket. While the distance observed between Cα of W496 and K1060 is clearly increased in F508del-CFTR (D), a significant portion of F508del conformations exhibits a decreased distance between F494 and W1063 (E).

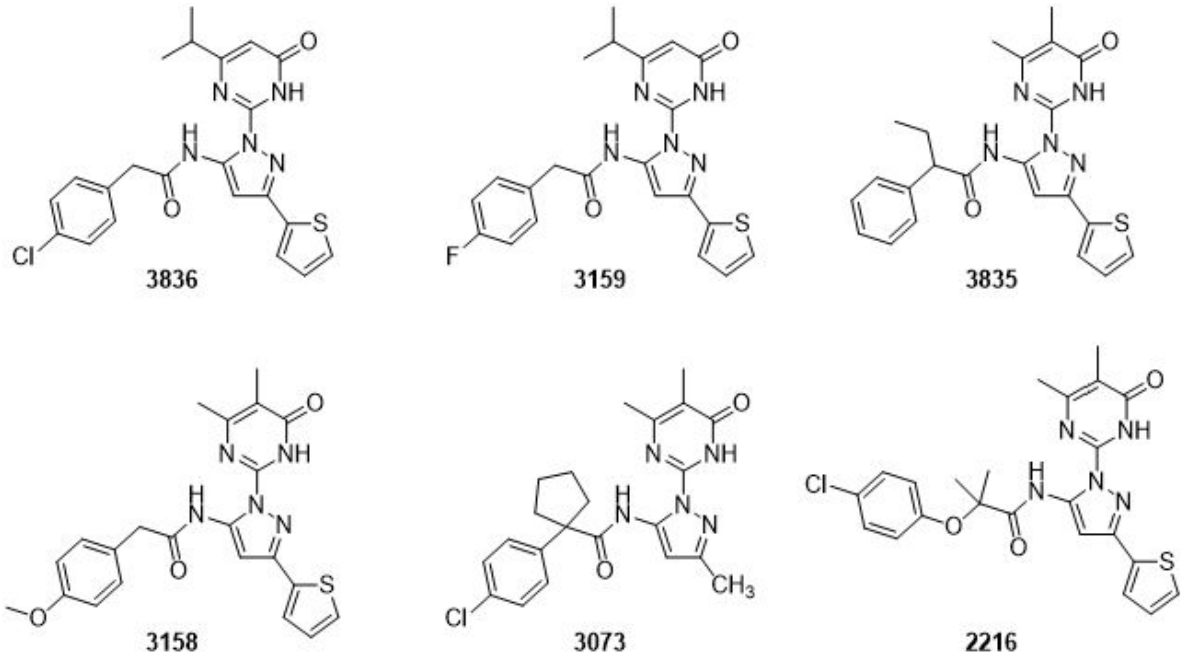

Figure S3. Commercially available compounds added to the training set for computing the 3D-QSAR model.

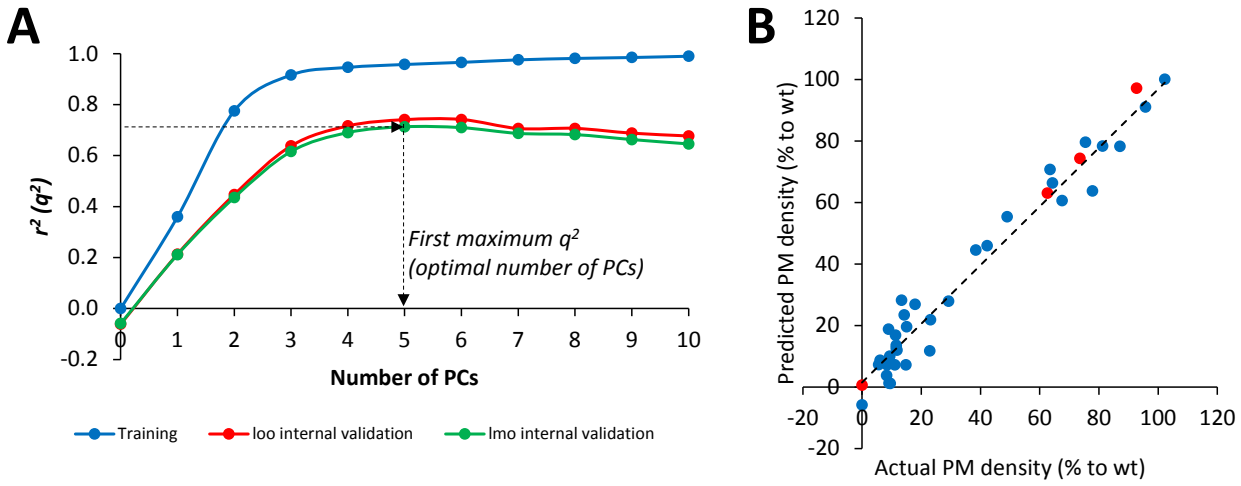

Figure S4. Statistics of the computed 3D-QSAR model. (A) correlation in training (r^2) and in internal validation (q^2) as a function of the number of principal components (PCs). The optimal number of PCs (5) has been chosen basing on the first maximum value of q^2. (B) correlation between actual and predicted PM density for the model with 5 PCs. Blue dots indicate the training set. Red dots indicate the 4 new compounds (**37**-**40**) not included in the training set.

Method S1: List of commands used to compute the 3D-QSAR model

box outgap=2

calc_field type=vdw

calc_field type=mm_ele diel_dep=DIST diel_const=4 smooth_probe=YES

cutoff type=min level=-10

cutoff type=max level=10

zero type=all level=0.05

sdcut level=0.1

scale_x_vars type=BUW

pls pc=10

cv pc=10 type=loo

cv pc=10 type=lmo groups=8 runs=20

srd pc=5 collapse=YES critical_distance=1 collapse_distance=2 type=WEIGHTS

ffdsel pc=5 type=lmo runs=20 percent_dummies=20 use_srd_groups=YES combination_variable_ratio=2 fold_over=NO

remove_x_vars type=FFDSEL

nlevel

remove_x_vars type=NLEVEL

scale_x_vars type=BUW

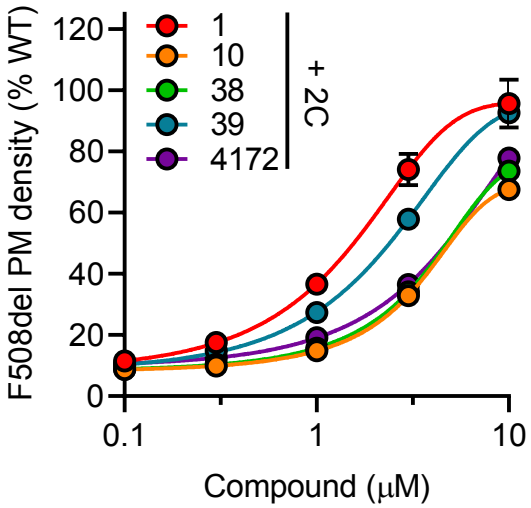

Figure S5. Dose-response curves reporting the 3xHA-F508del-CFTR PM density of the indicated compounds (24 hours, 37°C incubation) in combination with 2C (VX-809 and 3151, 3μM and 10μM, respectively) determined by PM-ELISA assay.

Compound	PM density EC_{50} (μM)	Function EC_{50} (μM)
1	1.79 ± 0.32	0.73 ± 0.38
10	6.03 ± 3.12	6.18 ± 3.21
38	6.16 ± 3.69	4.07 ± 2.28
39	3.05 ± 0.82	2.15 ± 1.01
4172	6.83 ± 0.86	1.85 ± 0.21

Table S2. EC_{50} values for the measured CFTR plasma membrane density (ELISA assay) and CFTR function (YFP quenching kinetic) curves. Data are reported as means ± s.e.m. of at least three independent experiments.

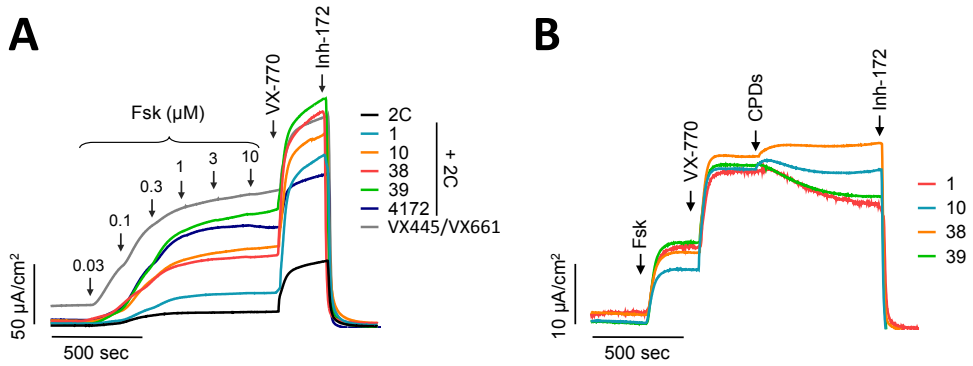

Figure S6. Chronic and acute effect on the function of F508del-CFTR. (A) Traces for the effect of indicated corrector combinations (10μM compounds + 2C; 2μM VX-445 / 3μM VX-661) on the Isc of F508del CFTR in CFBE41o - cells. CFTR-mediated short circuit currents (Isc) were induced by sequential acute addition of increasing concentrations of forskolin (Fsk) and VX-770 (10 μM each), followed by CFTR inhibition with CFTR inh-172 (20 μM) in the presence of a basolateral to apical chloride gradient after basolateral permeabilization with amphotericin B. (B) Traces for acute effect of correctors to the 20 μM forskolin activated and 10 μM VX-770 potentiated Isc of 2C rescued F508del-CFTR.

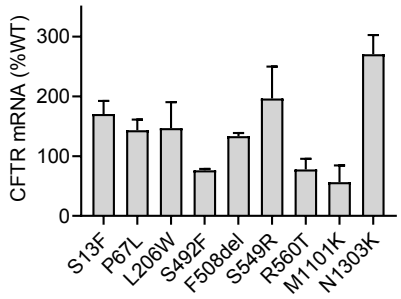

Figure S7. Mutant CFTR mRNA expression in CFBE41o- determined by qPCR and expressed as percent of wt-CFTR mRNA level (n = 3). Data in are means ± s.e.m. of three independent experiments

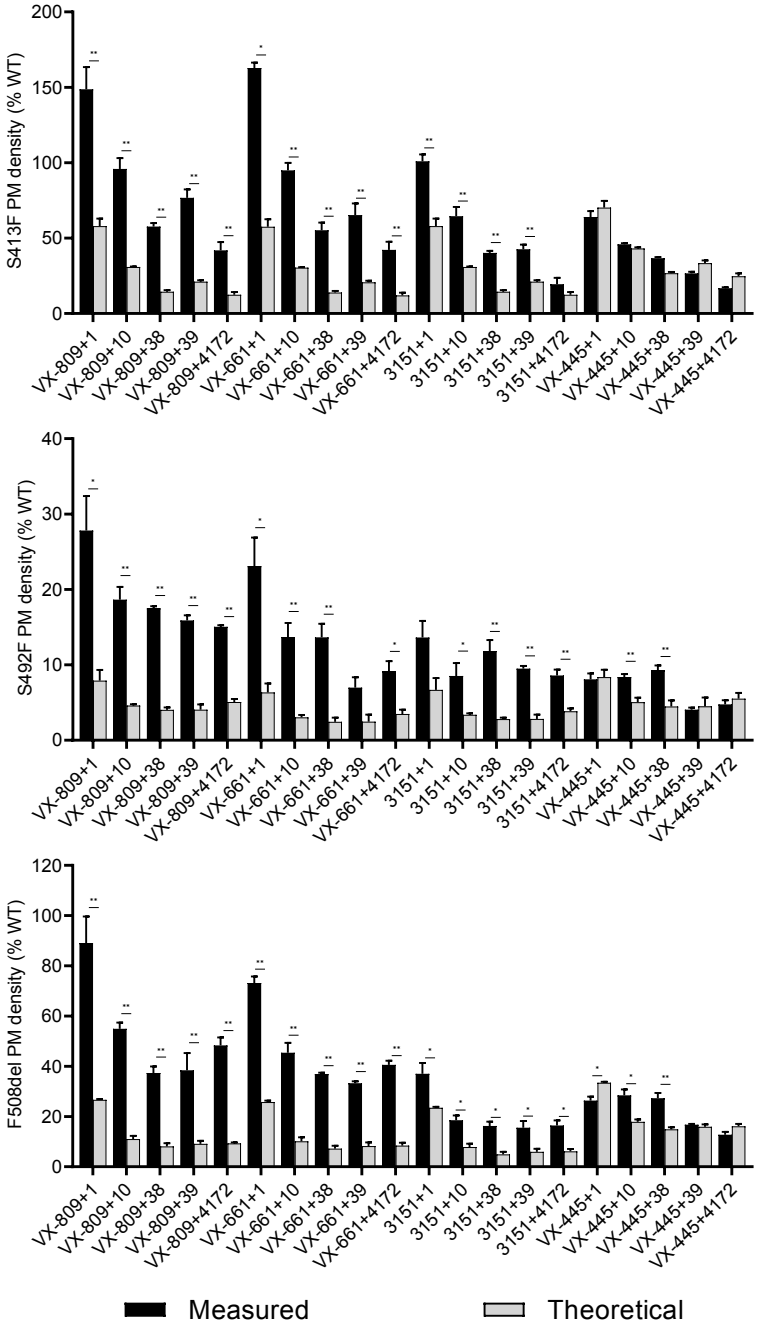

Figure S8. Allosteric correction of CFTR rare mutations. S13F (top), S492F (middle), and F508del (bottom) -CFTR PM density, measured by cell surface ELISA in CFBE41o- cells upon exposure to the reported dual corrector combinations (24 h, VX-445 = 2 μM; VX-809 and VX-661 = 3 μM; novel compounds and **3151** = 10 μM,) in comparison to the calculated additivity of single corrector effects (n=3). Data are means ± s.e.m. of three independent experiments. *p <0.05, **p < 0.01 by two-tailed Student's t-test between experiments pairs.

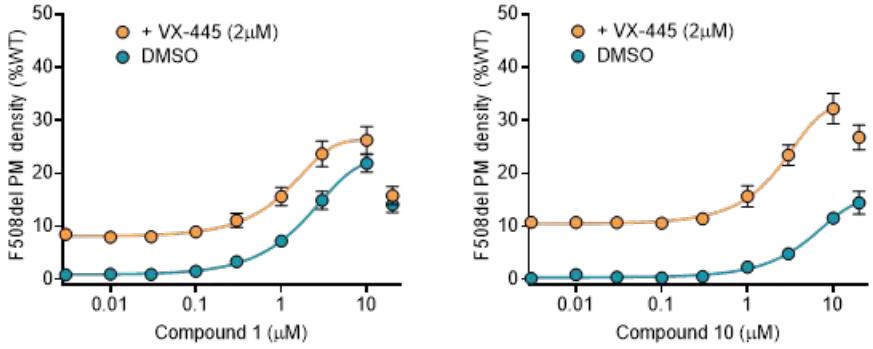

Figure S9. Additive effect of VX-445 (2 μM) on the dose-dependent corrector effect elicited by 1 (left) or 10 (right) on F508del-CFTR PM density (n=3). The maximum effects (% if the wt) as well as the EC50 values are reported in the graphs.

Appendix: ^{1}H and ^{13}C NMR spectra for tested compounds

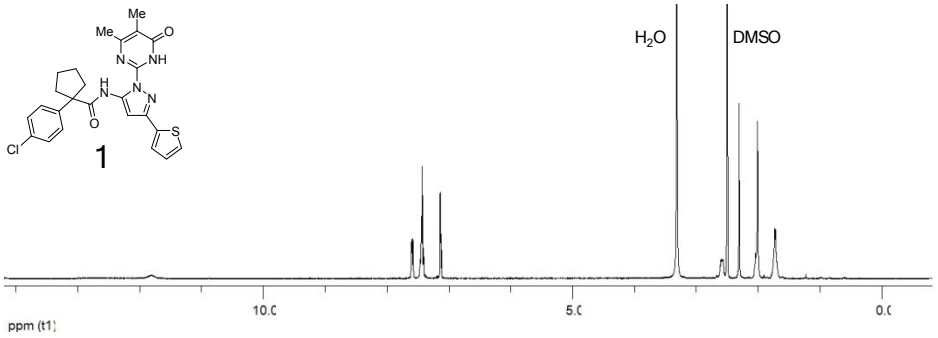

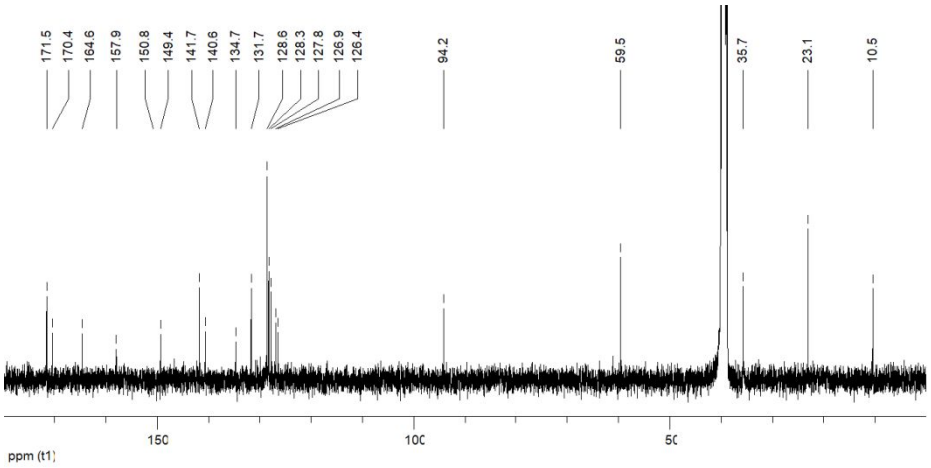

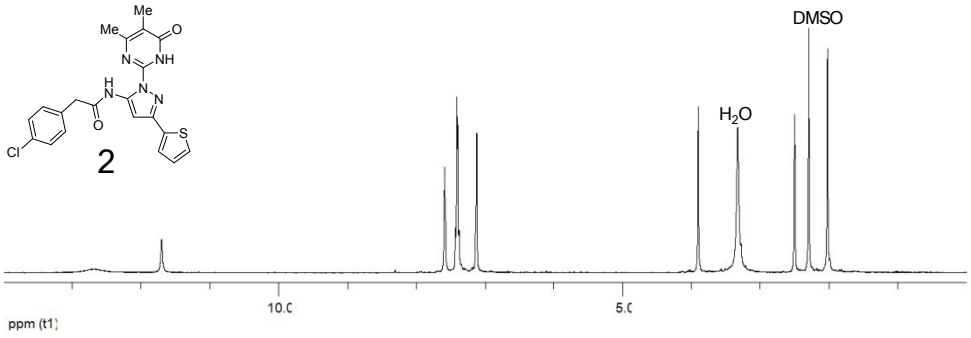

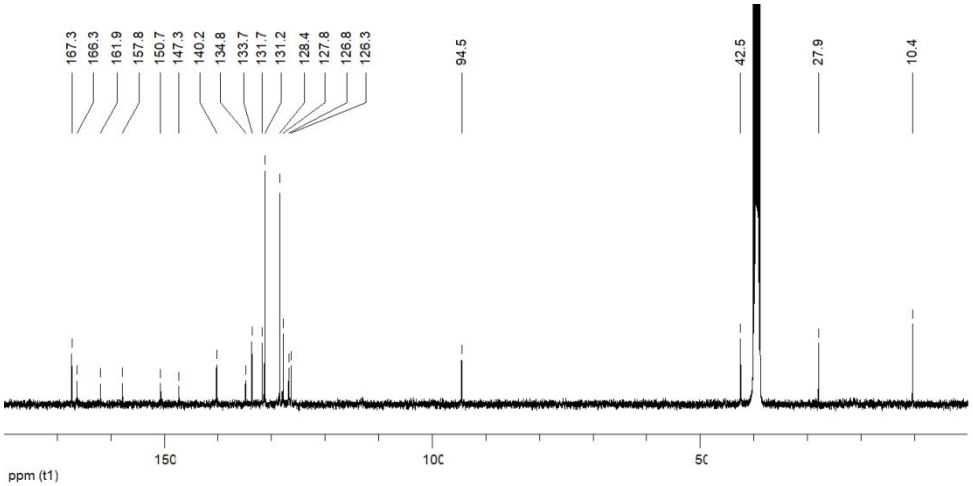

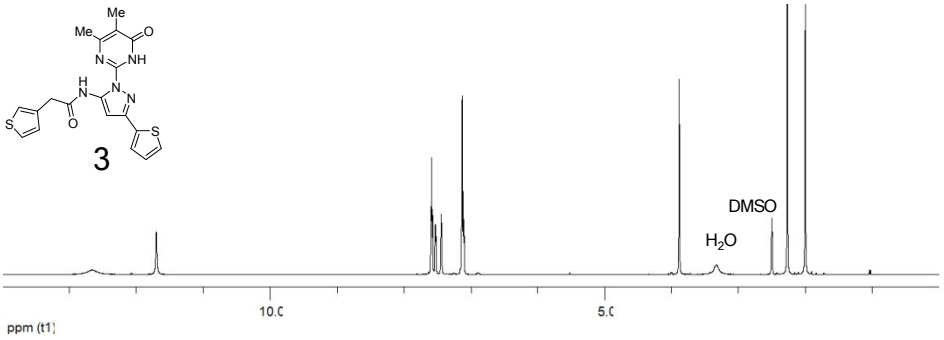
Me
Me
O
N
NH
H
N
N
N
O
S
S
3
DMSO
H2O
10.0
5.0
ppm (t1)

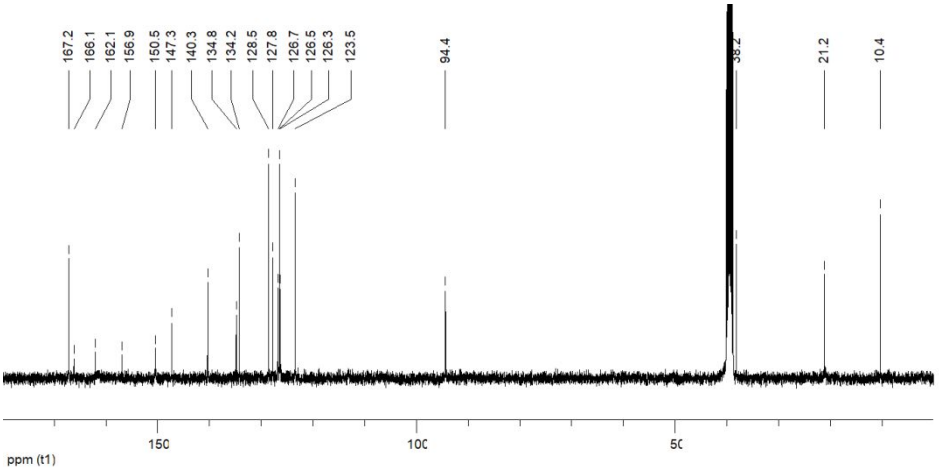
167.2
166.1
162.1
156.9
150.5
147.3
140.3
134.8
134.2
128.5
127.8
126.7
126.5
126.3
123.5
94.4
38.2
21.2
10.4
150
100
50
ppm (t1)

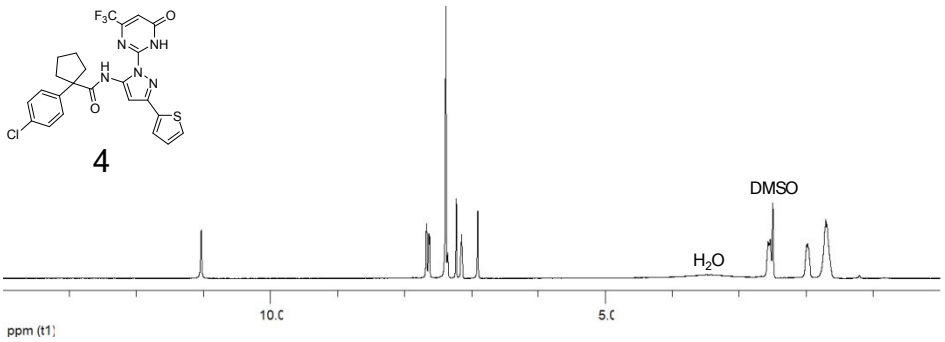
F3C
O
N
NH
H
N
N
O
Cl
S
4
DMSO
H2O
10.0
5.0
ppm (t1)

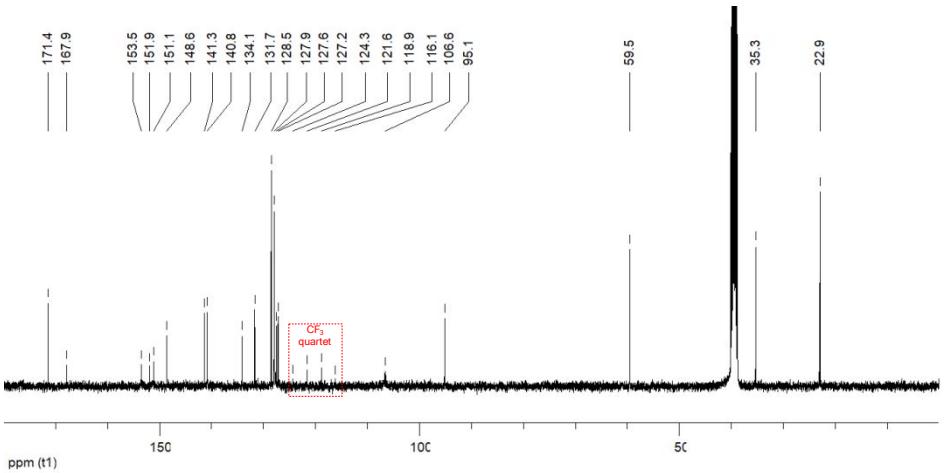
171.4
167.9
153.5
151.9
151.1
148.6
141.3
140.8
134.1
131.7
128.5
127.9
127.6
127.2
124.3
121.6
118.9
116.1
106.6
95.1
59.5
35.3
22.9
CF3 quartet
150
100
50
ppm (t1)

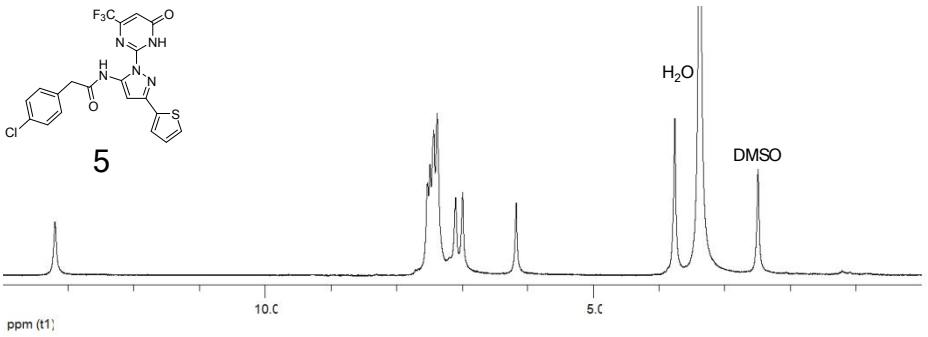
5
H2O
DMSO
ppm (t1)

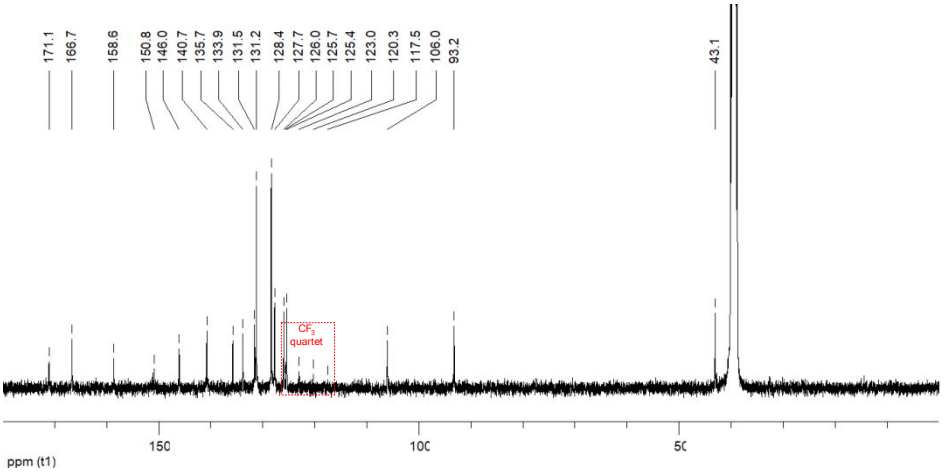
171.1
166.7
158.6
150.8
146.0
140.7
135.7
133.9
131.5
131.2
128.4
127.7
126.0
125.7
125.4
123.0
120.3
117.5
106.0
93.2
43.1
CF3 quartet
ppm (t1)

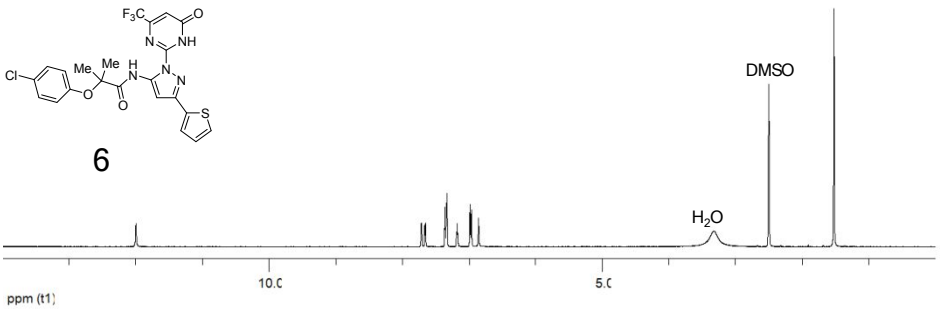
6
DMSO
H2O
ppm (t1)

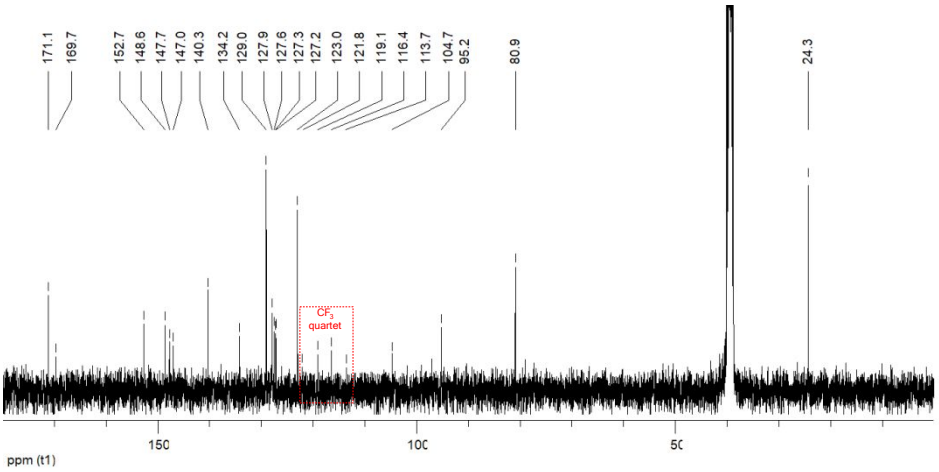
171.1
169.7
152.7
148.6
147.7
147.0
140.3
134.2
129.0
127.9
127.6
127.3
127.2
123.0
121.8
119.1
116.4
113.7
104.7
95.2
80.9
24.3
CF3 quartet
ppm (t1)

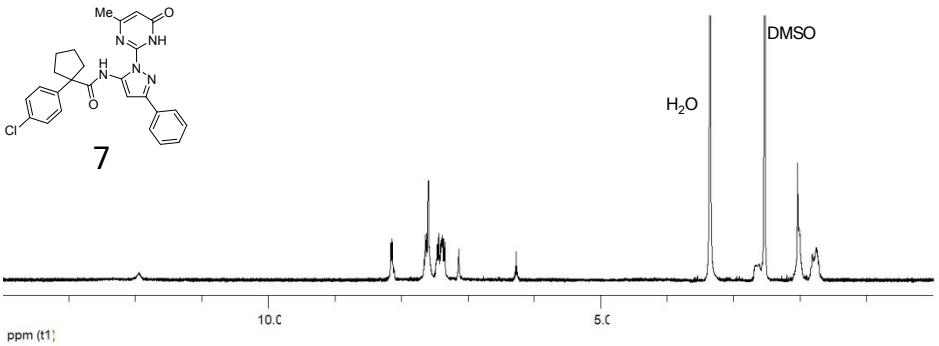
Me
O
NH
N
H
N
N
O
Cl
7
DMSO
H2O
10.0
5.0
ppm (t1)

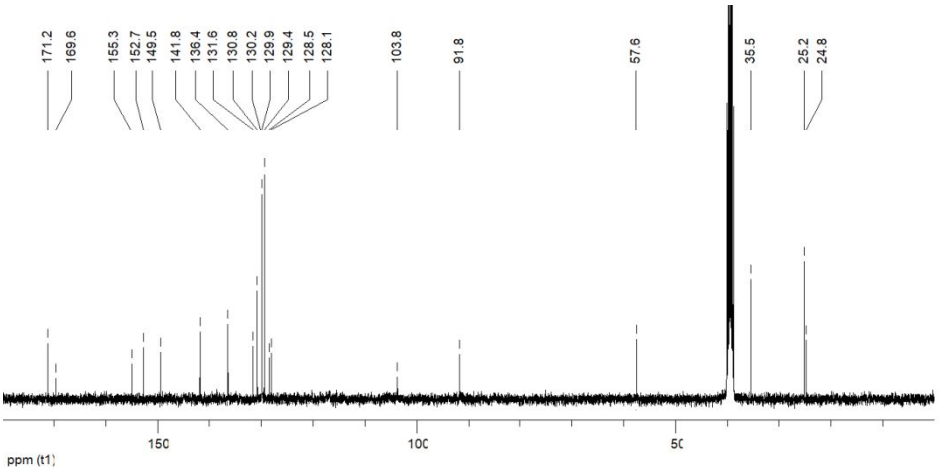
171.2
169.6
155.3
152.7
149.5
141.8
136.4
131.6
130.8
130.2
129.9
129.4
128.5
128.1
103.8
91.8
57.6
35.5
25.2
24.8
150
100
50
ppm (t1)

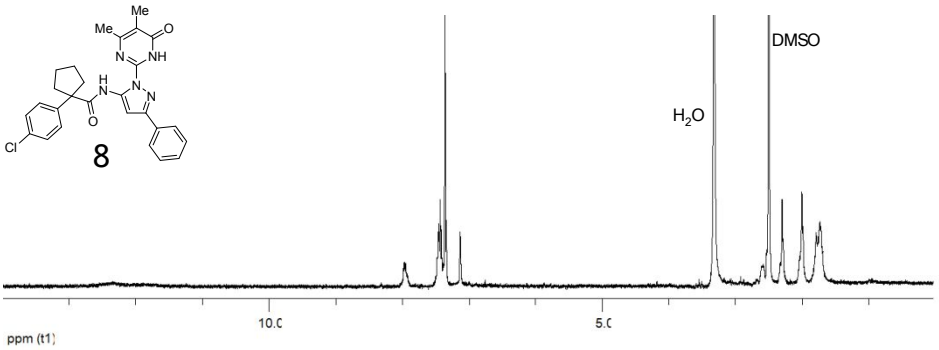
Me
Me
O
NH
N
H
N
N
O
Cl
8
DMSO
H2O
10.0
5.0
ppm (t1)

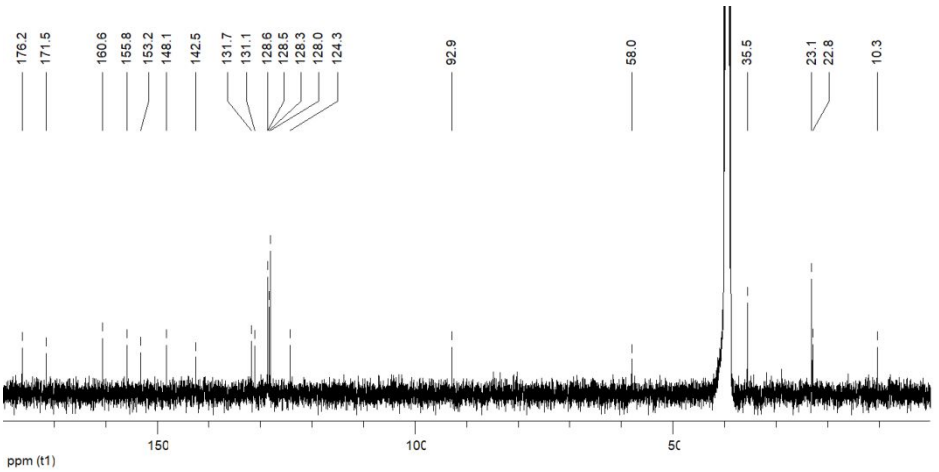
176.2
171.5
160.6
155.8
153.2
148.1
142.5
131.7
131.1
128.6
128.5
128.3
128.0
124.3
92.9
58.0
35.5
23.1
22.8
10.3
150
100
50
ppm (t1)

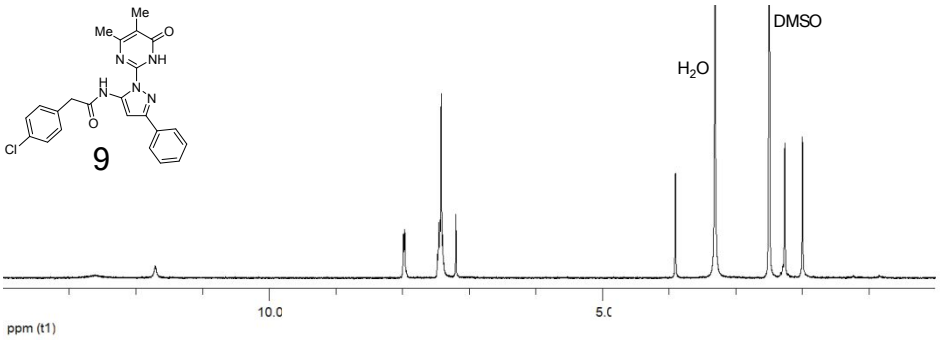
Me
Me
O
N
NH
H
N
N
O
Cl
9
DMSO
H2O
10.0
5.0
ppm (t1)

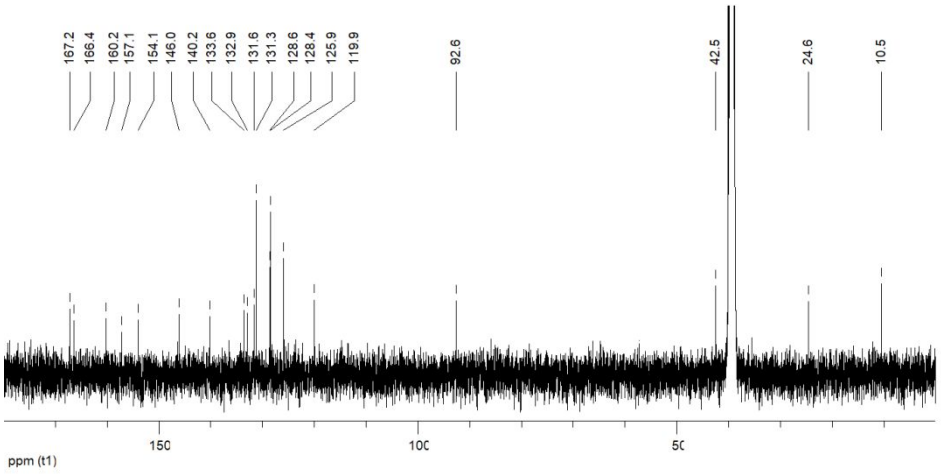
167.2
166.4
160.2
157.1
154.1
146.0
140.2
133.6
132.9
131.6
131.3
128.6
128.4
125.9
119.9
92.6
42.5
24.6
10.5
150
100
50
ppm (t1)

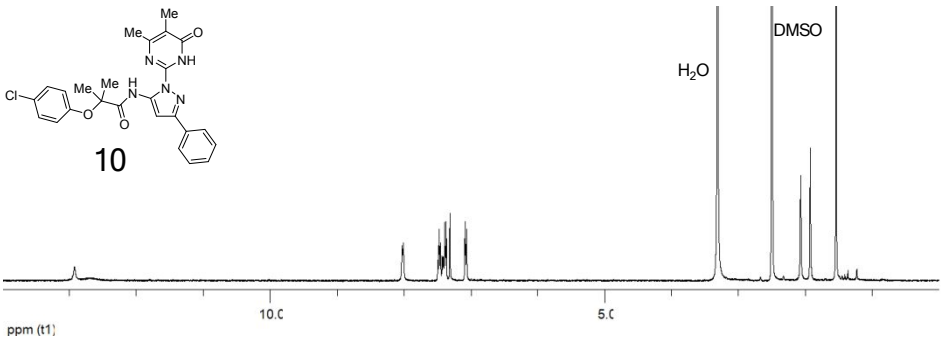
Me
Me
O
N
NH
Cl
Me
Me
H
N
N
O
O
10
DMSO
H2O
10.0
5.0
ppm (t1)

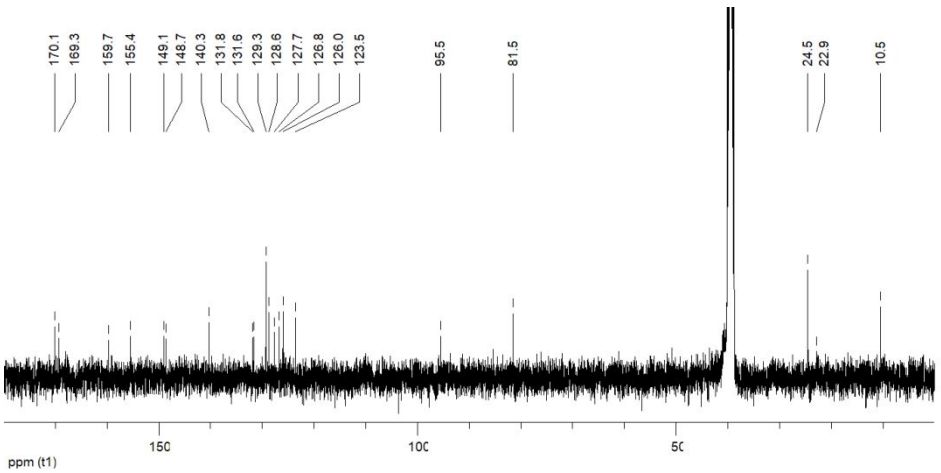
170.1
169.3
159.7
155.4
149.1
148.7
140.3
131.8
131.6
129.3
128.6
127.7
126.8
126.0
123.5
95.5
81.5
24.5
22.9
10.5
150
100
50
ppm (t1)

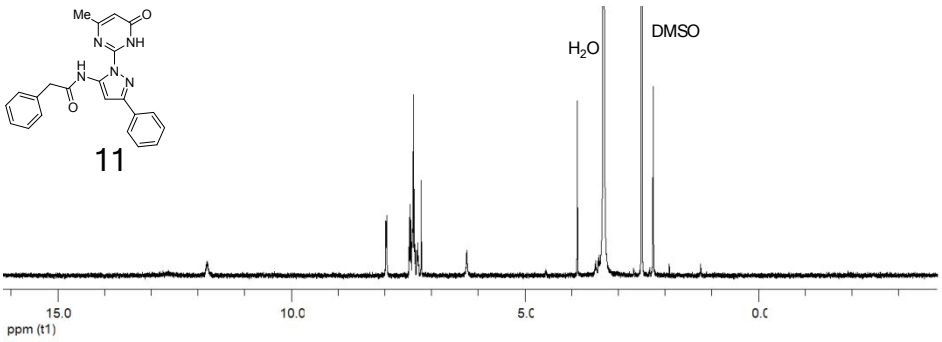
Me
O
N
NH
H
N
N
O
11
H2O
DMSO
15.0
10.0
5.0
0.0
ppm (t1)

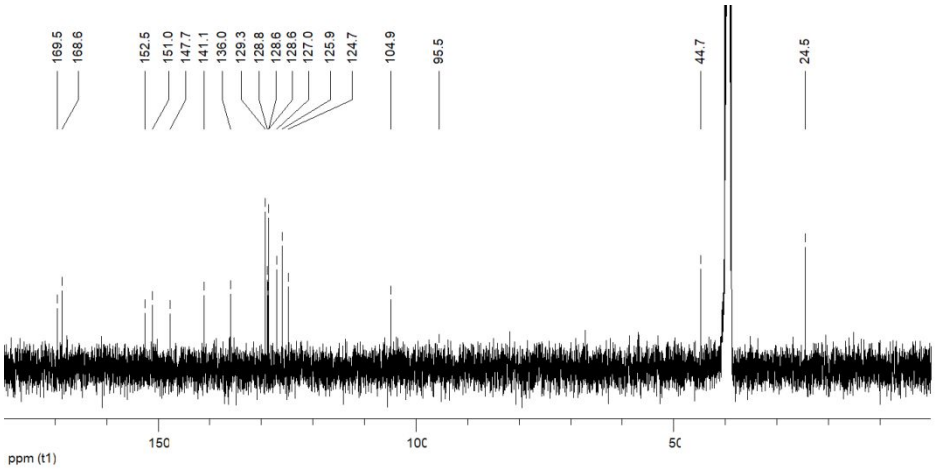
169.5
168.6
152.5
151.0
147.7
141.1
136.0
129.3
128.8
128.6
128.6
127.0
125.9
124.7
104.9
95.5
44.7
24.5
150
100
50
ppm (t1)

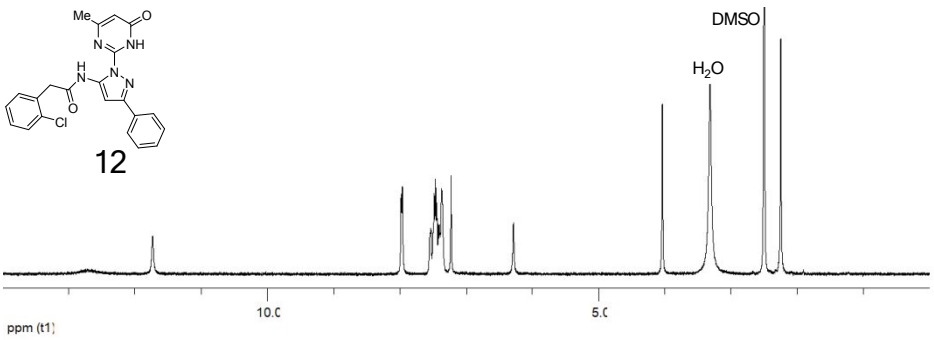
Me
O
N
NH
H
N
N
O
Cl
12
DMSO
H2O
10.0
5.0
ppm (t1)

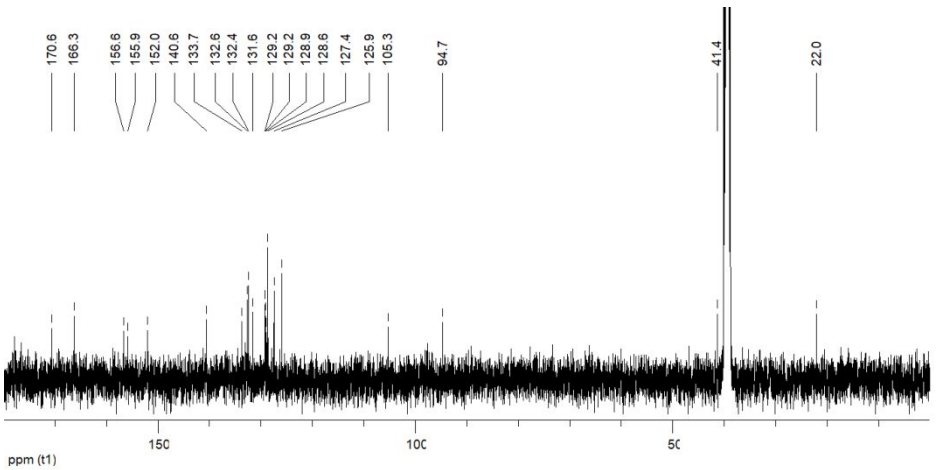
170.6
166.3
156.6
155.9
152.0
140.6
133.7
132.6
132.4
131.6
129.2
129.2
128.9
128.6
127.4
125.9
105.3
94.7
41.4
22.0
150
100
50
ppm (t1)

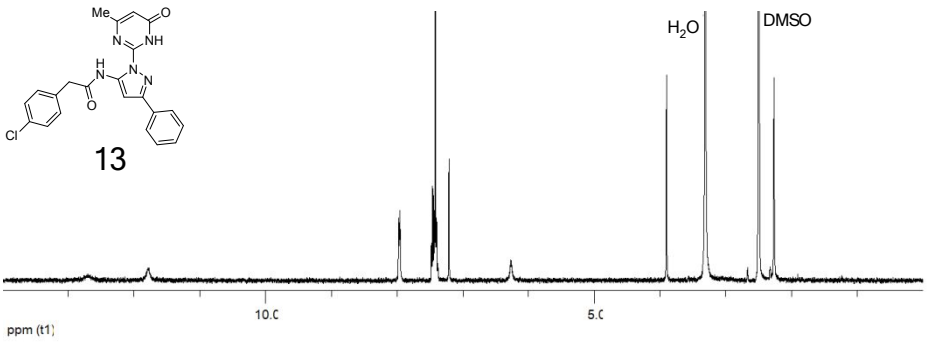
Me
O
NH
N
H
N
N
O
Cl
13
H2O
DMSO
10.0
5.0
ppm (t1)

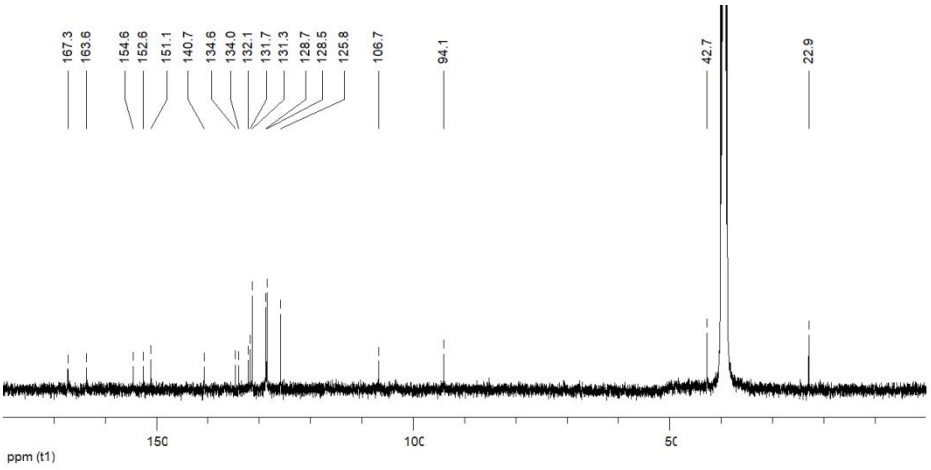
167.3
163.6
154.6
152.6
151.1
140.7
134.6
134.0
132.1
131.7
131.3
128.7
128.5
125.8
106.7
94.1
42.7
22.9
150
100
50
ppm (t1)

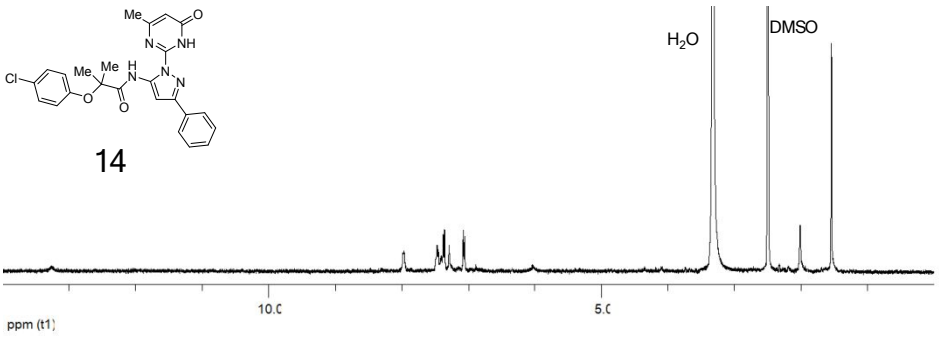
Me
O
NH
N
Me
Me
H
N
N
Cl
O
O
14
H2O
DMSO
10.0
5.0
ppm (t1)

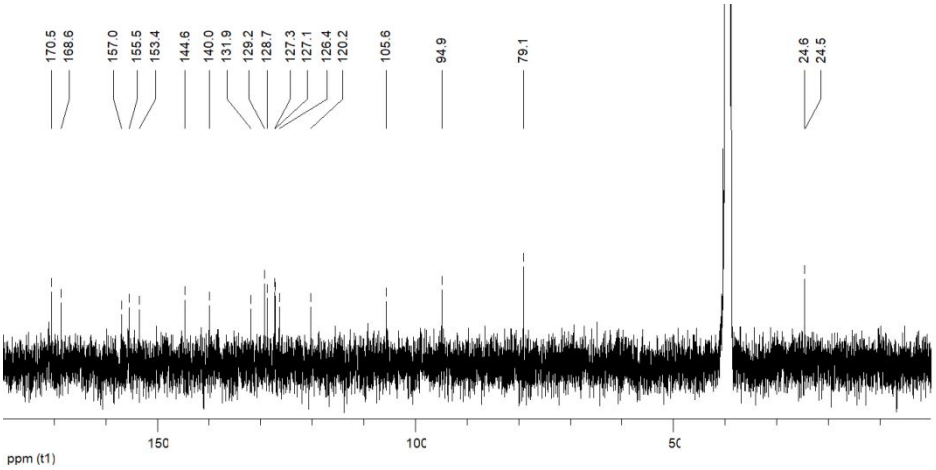
170.5
168.6
157.0
155.5
153.4
144.6
140.0
131.9
129.2
128.7
127.3
127.1
126.4
120.2
105.6
94.9
79.1
24.6
24.5
150
100
50
ppm (t1)

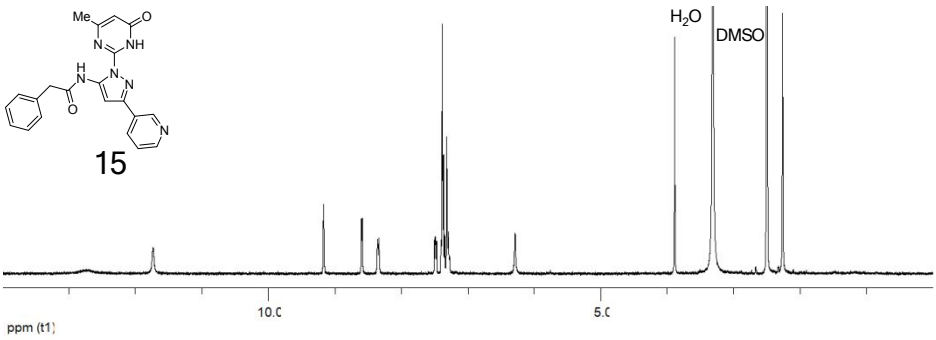
Me
O
N
NH
H
N
N
O
N
15
H2O
DMSO
10.0
5.0
ppm (t1)

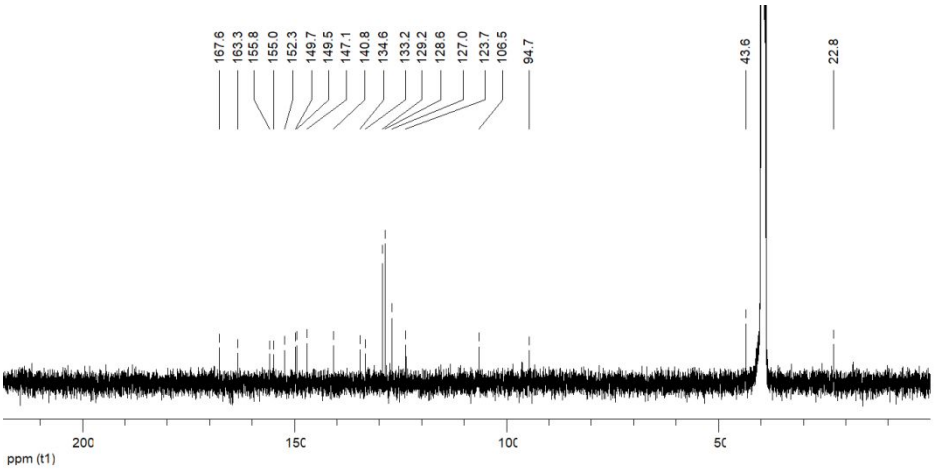
167.6
163.3
155.8
155.0
152.3
149.7
149.5
147.1
140.8
134.6
133.2
129.2
128.6
127.0
123.7
106.5
94.7
43.6
22.8
200
150
100
50
ppm (t1)

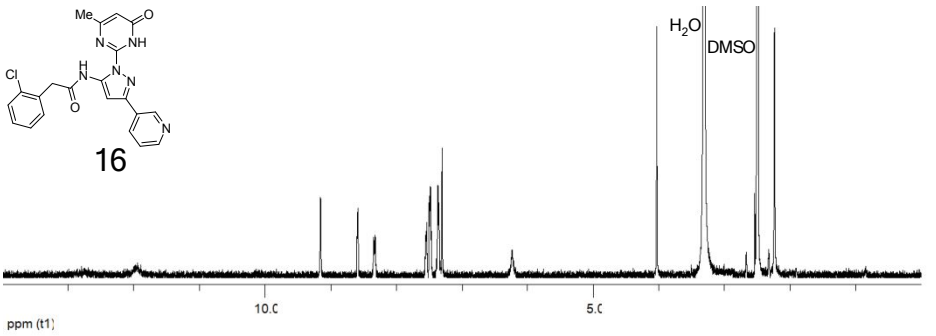
Me
O
N
NH
H
N
N
Cl
O
N
16
H2O
DMSO
10.0
5.0
ppm (t1)

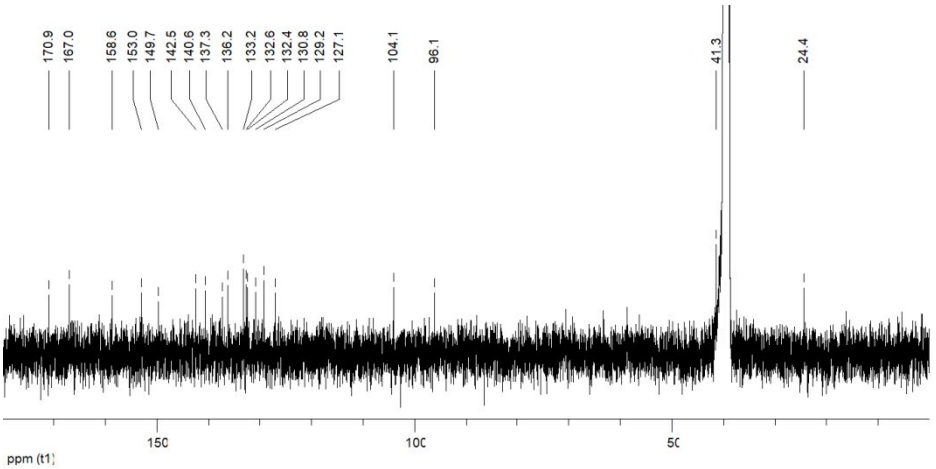
170.9
167.0
158.6
153.0
149.7
142.5
140.6
137.3
136.2
133.2
132.6
132.4
130.8
129.2
127.1
104.1
96.1
41.3
24.4
150
100
50
ppm (t1)

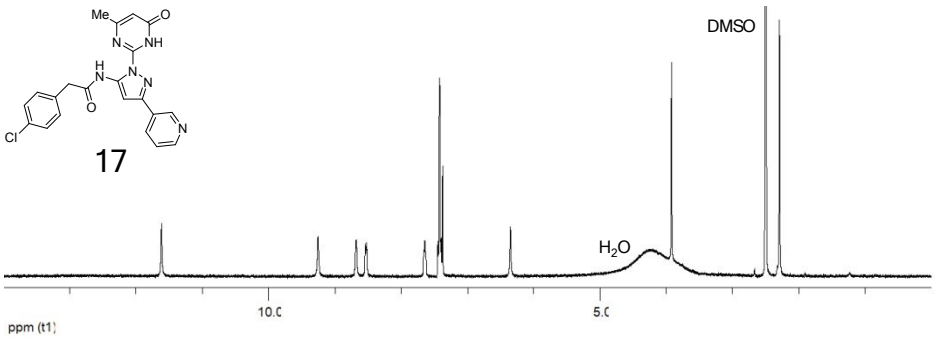
Me
O
NH
N
H
N
N
O
Cl
N
17
DMSO
H2O
10.0
5.0
ppm (t1)

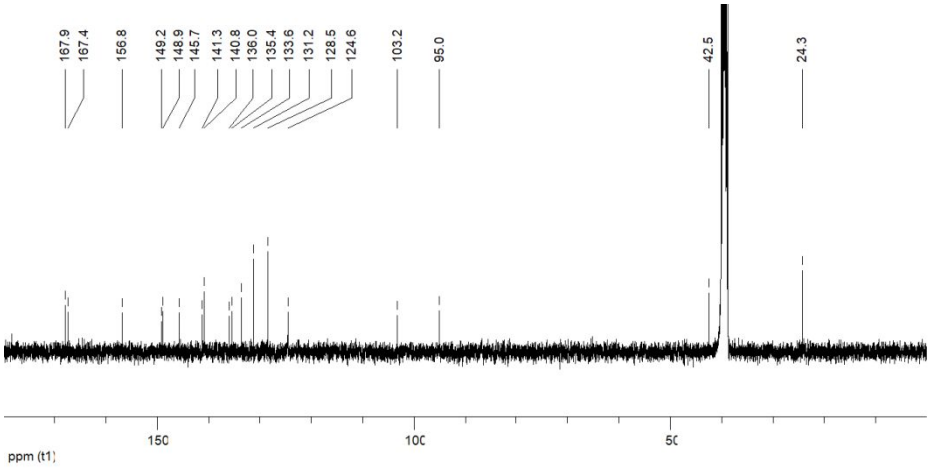
167.9
167.4
156.8
149.2
148.9
145.7
141.3
140.8
136.0
135.4
133.6
131.2
128.5
124.6
103.2
95.0
42.5
24.3
150
100
50
ppm (t1)

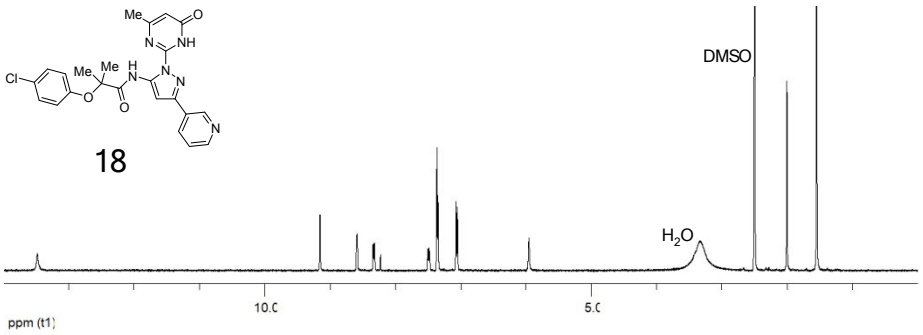
Me
O
NH
N
Cl
Me
Me
H
N
N
O
O
N
18
DMSO
H2O
10.0
5.0
ppm (t1)

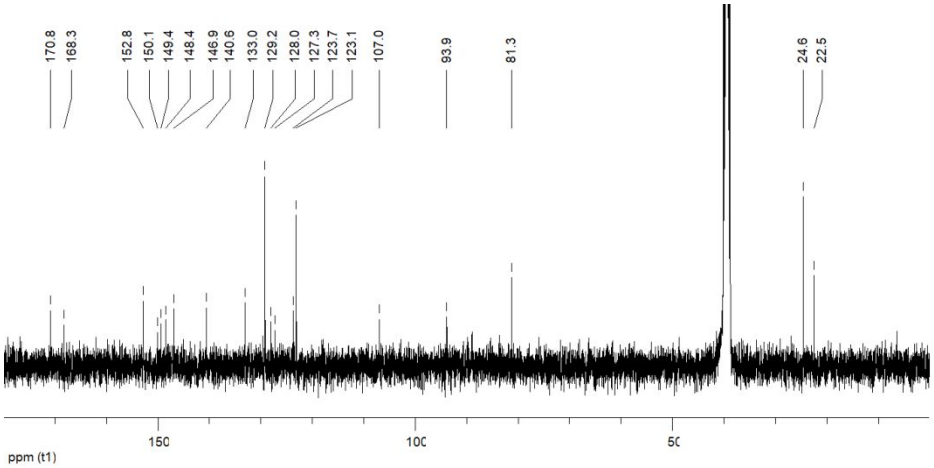
170.8
168.3
152.8
150.1
149.4
148.4
146.9
140.6
133.0
129.2
128.0
127.3
123.7
123.1
107.0
93.9
81.3
24.6
22.5
150
100
50
ppm (t1)

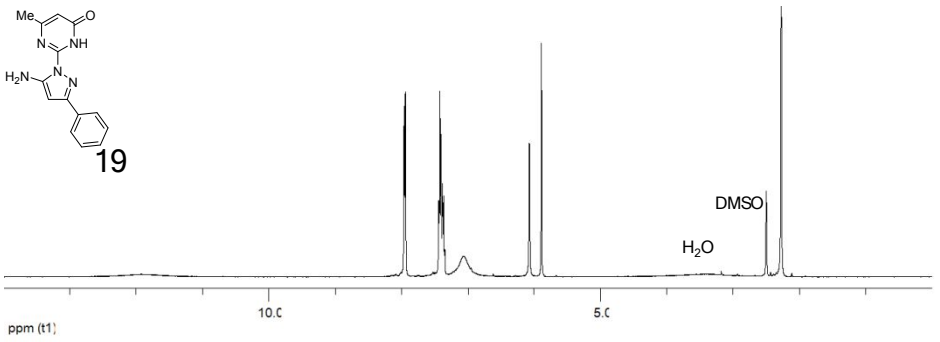
Me
O
N
NH
H2N
N
N
19
DMSO
H2O
10.0
5.0
ppm (t1)

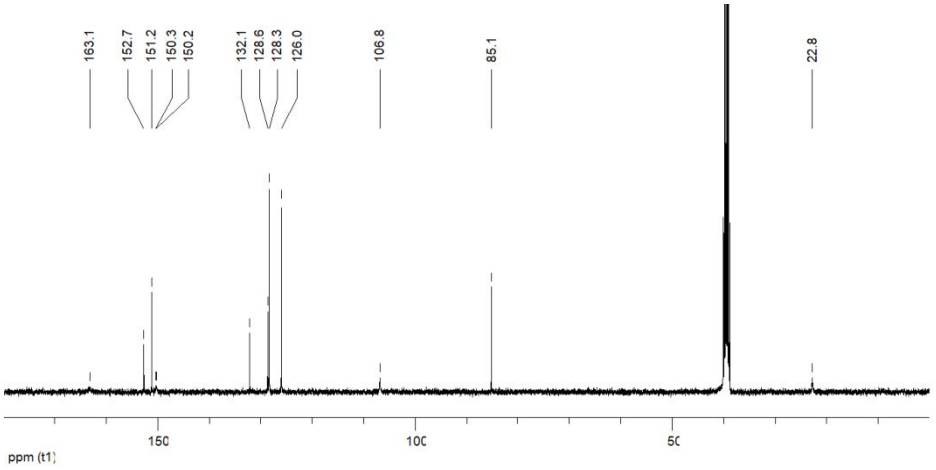
163.1
152.7
151.2
150.3
150.2
132.1
128.6
128.3
126.0
106.8
85.1
22.8
150
100
50
ppm (t1)

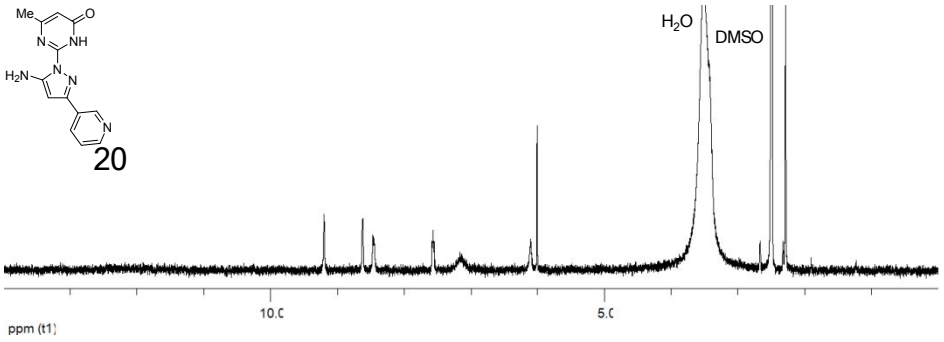
Me
O
N
NH
H2N
N
N
N
20
H2O
DMSO
10.0
5.0
ppm (t1)

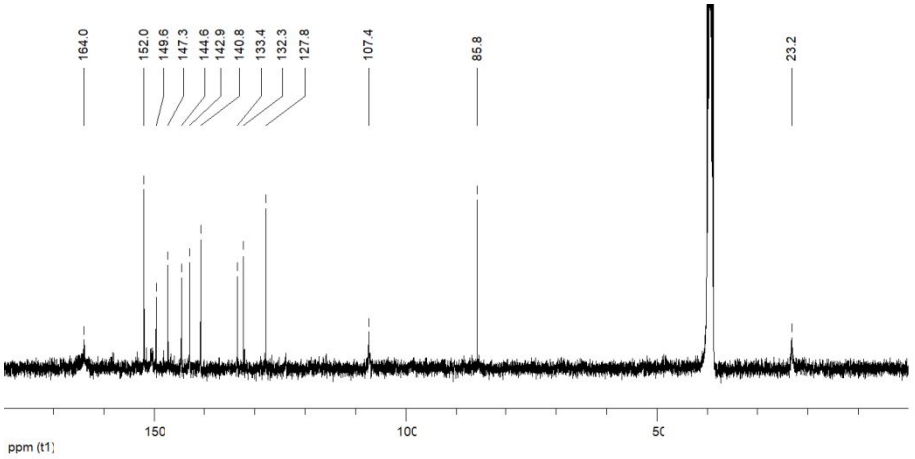
164.0
152.0
149.6
147.3
144.6
142.9
140.8
133.4
132.3
127.8
107.4
85.8
23.2
150
100
50
ppm (t1)

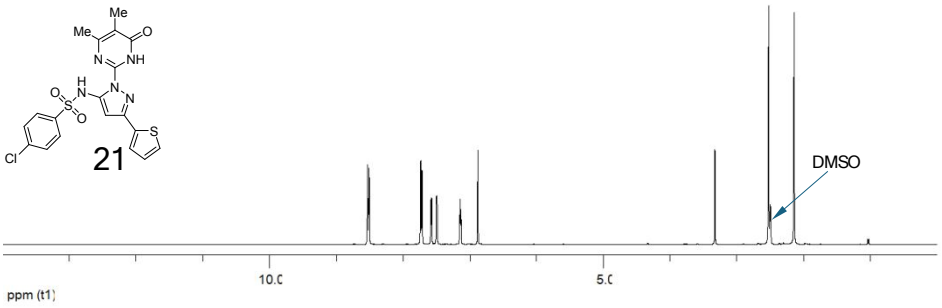
Me
Me
O
N
NH
H
N
N
N
O
S
O
Cl
S
21
DMSO
10.0
5.0
ppm (t1)

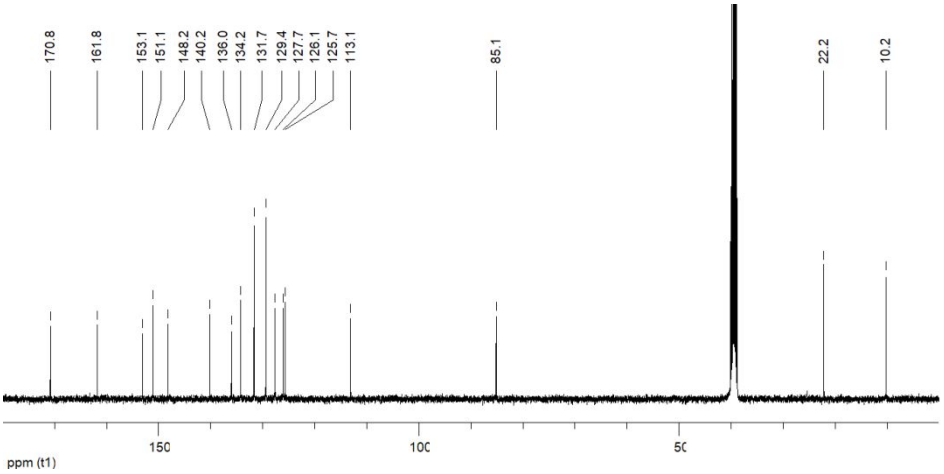
170.8
161.8
153.1
151.1
148.2
140.2
136.0
134.2
131.7
129.4
127.7
126.1
125.7
113.1
85.1
22.2
10.2
150
100
50
ppm (t1)

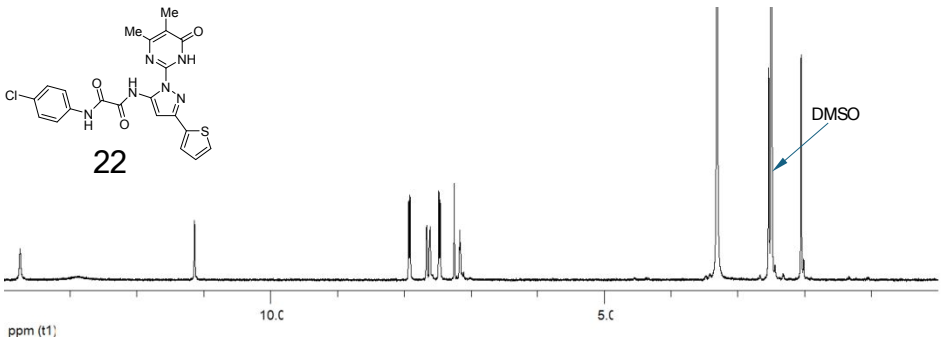
Me
Me
O
N
NH
Cl
O
H
N
N
N
H
N
O
S
22
DMSO
10.0
5.0
ppm (t1)

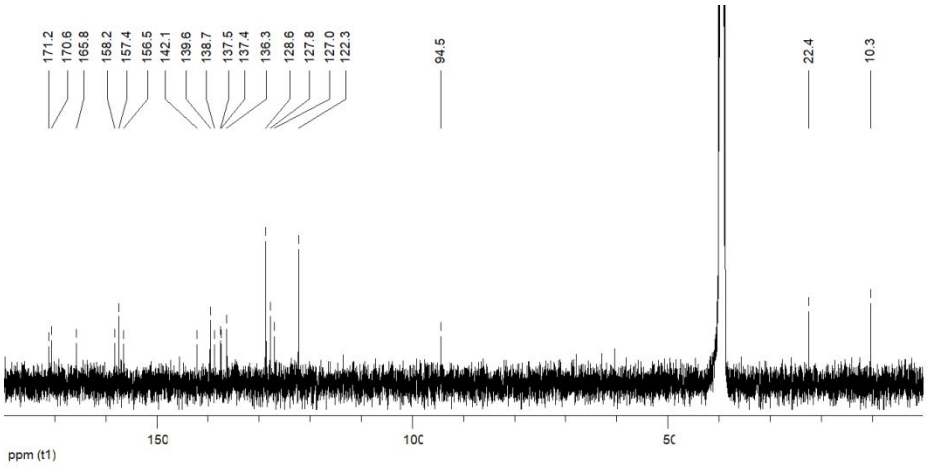
171.2
170.6
165.8
158.2
157.4
156.5
142.1
139.6
138.7
137.5
137.4
136.3
128.6
127.8
127.0
122.3
94.5
22.4
10.3
150
100
50
ppm (t1)

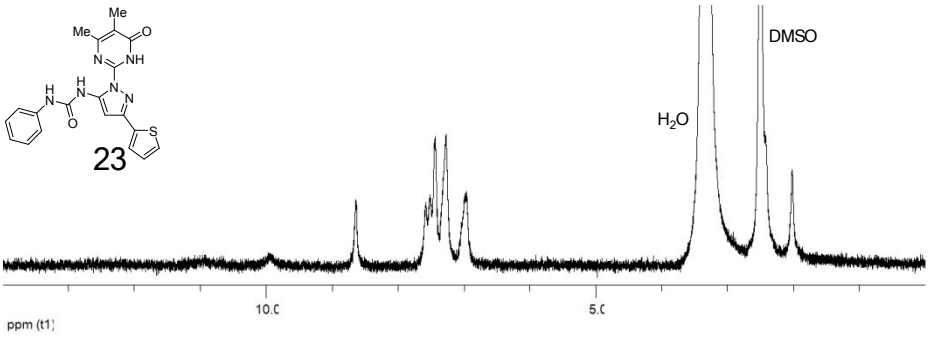
Me
Me
O
N
NH
H
N
N
N
H
N
O
S
23
DMSO
H2O
10.0
5.0
ppm (t1)

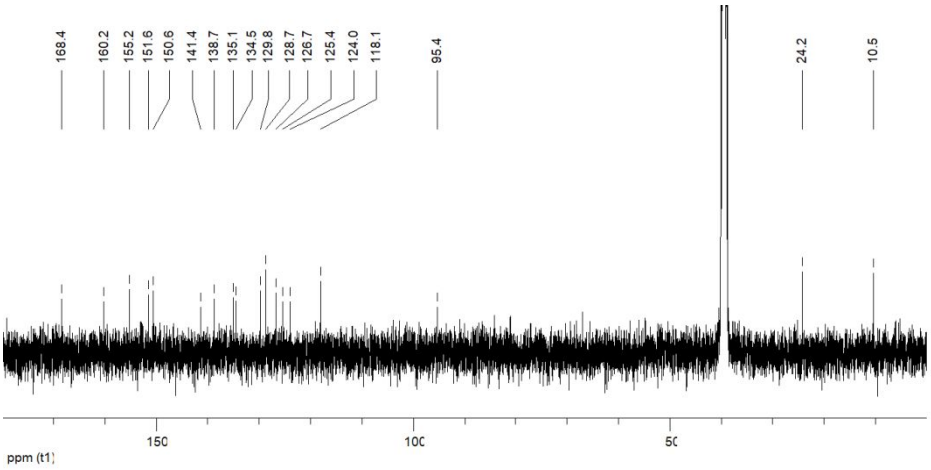
168.4
160.2
155.2
151.6
150.6
141.4
138.7
135.1
134.5
129.8
128.7
126.7
125.4
124.0
118.1
95.4
24.2
10.5
150
100
50
ppm (t1)

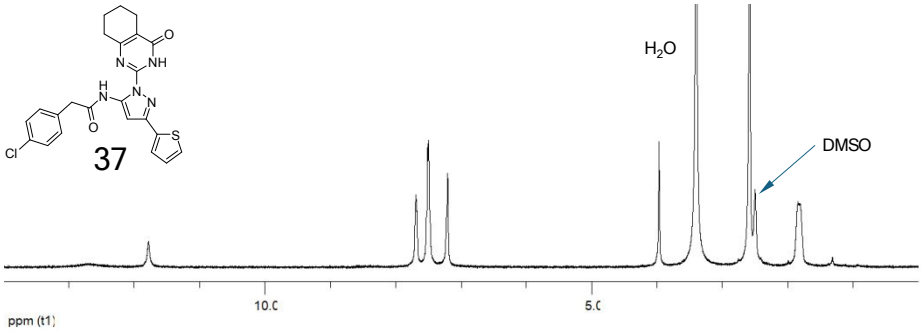
O
N
NH
H
N
N
N
O
Cl
S
37
H2O
DMSO
10.0
5.0
ppm (t1)

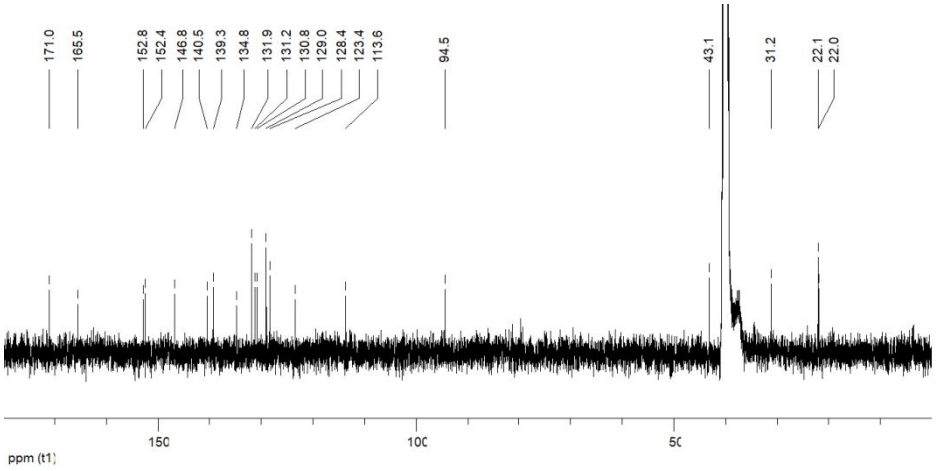
171.0
165.5
152.8
152.4
146.8
140.5
139.3
134.8
131.9
131.2
130.8
129.0
128.4
123.4
113.6
94.5
43.1
31.2
22.1
22.0
150
100
50
ppm (t1)

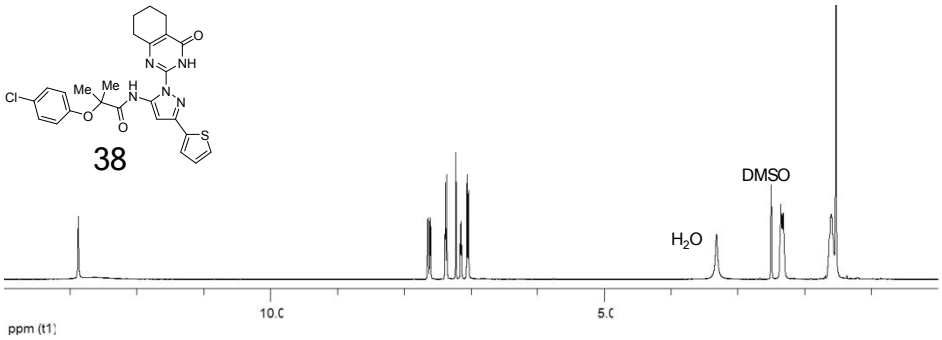
38
DMSO
H2O
10.0
5.0
ppm (t1)

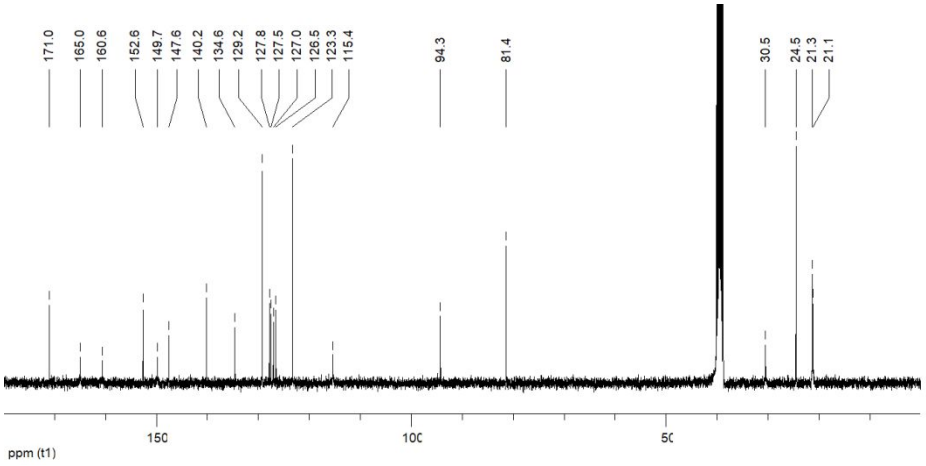
171.0
165.0
160.6
152.6
149.7
147.6
140.2
134.6
129.2
127.8
127.5
127.0
126.5
123.3
115.4
94.3
81.4
30.5
24.5
21.3
21.1
150
100
50
ppm (t1)

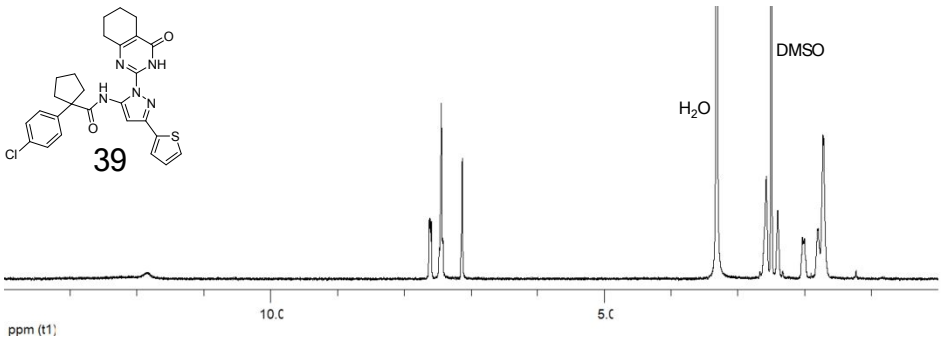
39
DMSO
H2O
10.0
5.0
ppm (t1)

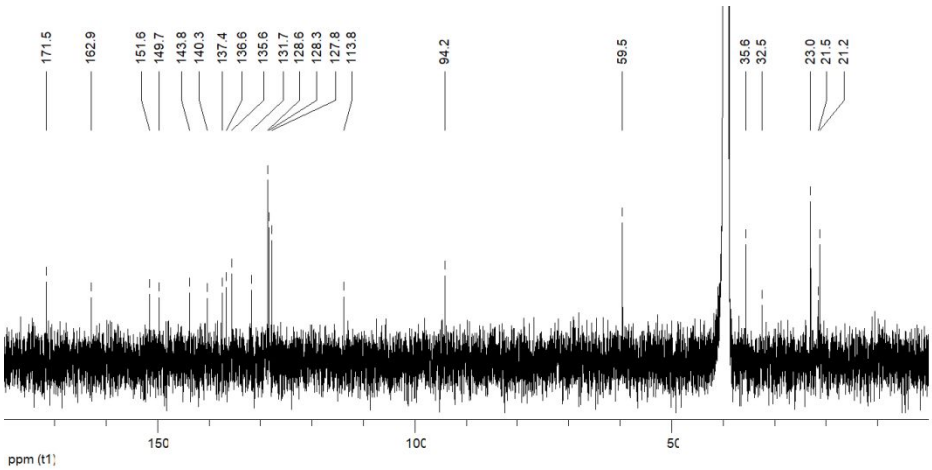
171.5
162.9
151.6
149.7
143.8
140.3
137.4
136.6
135.6
131.7
128.6
128.3
127.8
113.8
94.2
59.5
35.6
32.5
23.0
21.5
21.2
150
100
50
ppm (t1)